IJFANS INTERNATIONAL JOURNAL OF FOOD AND NUTRITIONAL SCIENCES
ISSN PRINT 2319 1775 Online 2320 7876
 Journal Volume 12, Iss 07, 2023

Design and Performance Enhancement of Miniaturized 1 x 4 Antipodal Vivaldi Antenna for 5G Communication Applications

POTHUREDDY GOWTHAMI[1*] , NALUKURTHI SUMALATHA[2]

[1,2] Department of ECE, Sri Venkateswara University College of Engineering, SV University, Tirupati 517502, AP, INDIA

Abstract— This paper presents the design of a miniaturized 1 x 4 Antipodal Vivaldi Antenna (AVA) tailored for 5th generation (5G) communication applications. The proposed AVA, measuring 28.8 mm x 24 mm x 0.254 mm, is fabricated using Rogers RT5880 substrate. Initially, a 1 x 4 AVA array (AVA-A) with slots between antenna elements is designed, operating over three frequency bands (24.91 GHz to 33.18 GHz, 34.95 GHz to 36.58 GHz, and 38.34 GHz to 39.38 GHz) with gains ranging from 8.47 dB to 12.63 dB. The performance of AVA-A is further improved by incorporating corrugations, resulting in AVA-A with corrugations (AVA-AC). AVA-AC exhibits enhanced gain, bandwidth, and front-to-back ratio, providing nearly constant gain of 8.2 dB to 13.2 dB over the 24.04 GHz to 40.85 GHz frequency range, including key bands of the 5G communication spectrum (24.25 GHz to 27.5 GHz, 31.8 GHz to 33.4 GHz, and 37 GHz to 40.5 GHz). Moreover, AVA-AC demonstrates stable radiation patterns across its entire operating range, rendering it suitable for integration into 5G communication devices.

Index Terms—Antipodal Vivaldi Antenna (AVA), Array, Miniaturized size, Enhanced gain, Stable radiation pattern

I. INTRODUCTION

The proliferation of wireless communication devices demands for wider bandwidth, stable radiation pattern, and enhanced gain. The AVA is the panacea of all these requirements which can operate at higher frequencies, raises the gain and provides stable radiation pattern [1], [2]. Due to rapid growth of wireless communication devices and their requirements, Federal Communications Commission (FCC) decided to launch high frequency bands for 5G communications which includes frequency bands near to 30 GHz, 40 GHz, 50 GHz, 70 GHz, and 80 GHz. This paper includes the AVA design for 31.8 GHz to 33.4 GHz, 31.8 GHz to 33.4 GHz, and 37 GHz to 40.5

ISSN PRINT 2319 1775 Online 2320 7876
 Journal Volume 12, Iss 07, 2023

GHz frequency bands of 5G communication devices. A concise review on AVA shows that the design of a compact AVA for 5G communication devices is the daunting task. The different enhancement techniques like metamaterial [3], [4], corrugations [5], [6], slots [7], [8], balanced AVA [9], [10], parasitic patch [11], [12], array [13], [14], and multiple input multiple output (MIMO) [15] can be used to enhance the AVA performance parameters. But, the parasitic patch which is incorporated in between two flares of AVA, increases the size of an antenna. Also, the design and fabrication of balanced AVA (which contains three layers of flares - two conductors and one ground) is complex. Further, AVA with metamaterial or MIMO design is the challenging task. Moreover, corrugation contributes to increase front to back ratio of AVA. As, the single AVA cannot meet the required specifications of 5G antenna, AVA array is required to be implemented [16]–[18].

In [19], 1 x 5 AVAarray with corrugation is implemented for medical imaging applications. The poor polarization of AVA array can be overcome by using balanced AVA array at the cost of increased complexity [20]. Further, AVA array with dielectric rod gives low insertion loss, enhanced isolation, and stable radiation pattern [21]. As aforementioned, one or more enhancement techniques can be used to enhance performance parameters of AVA. In [22], AVA array with corrugations, dielectric lens and substrate integrated waveguide (SIW) are used to boost up the gain to 23 dB. This paper contains the design of 1 x 4 AVA array with corrugations (AVA-AC) for 5G applications. The details AVA-AC design in explained in section II. The importance the AVA-AC is proved with the help of simulation results which is given in section III and the conclusion of the designed AVA-AC is given in section IV.

II. AVA-AC DESIGN

The AVA-AC is designed on Rogers RT5880 substrate and its size is 28.8 mm X 24 mm x 0.254 mm which is very compact. Initially, 1 x 4 AVA array is designed as shown in figure 1(a) and then to enhance the gain and front to back ratio, the rectangular corrugations are incorporated as shown in figure 1(b). The dimensions of corrugations are optimized by using simulation software High Frequency Structure Simulator (HFSS, version 19). The designed AVA-AC contains four upper flares of copper metal which acts as a conductor and four lower flares of copper metal which acts as a ground.

ISSN PRINT 2319 1775 Online 2320 7876
 Journal Volume 12, Iss 07, 2023

The equations of inner and outer exponential curves are given below [23]:

$$Y) =) \pm (C1e^{ax}) +) C2) \qquad (1)$$

where C_1 and C_2 are given by,

$$C1 = {}^{y2 - y1}/_{e2 - e^{ax1}} \qquad (2)$$

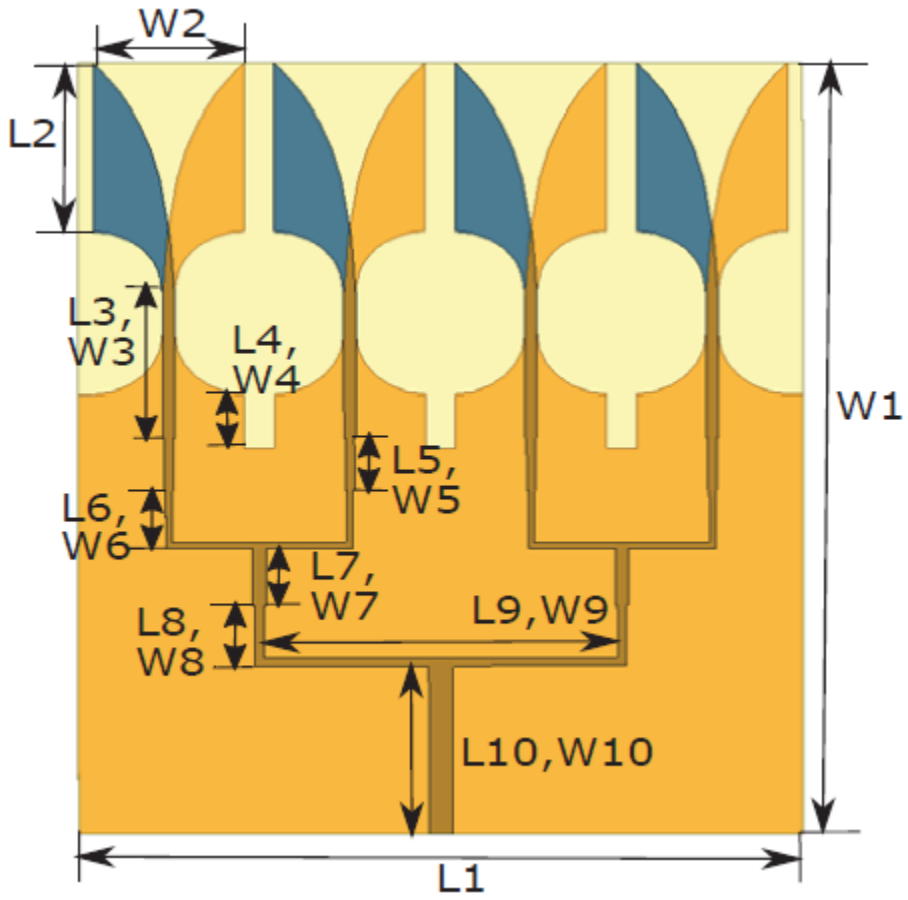

Fig.1: (a) Design of AVA array (AVA-A)

ISSN PRINT 2319 1775 Online 2320 7876
 Journal Volume 12, Iss 07, 2023

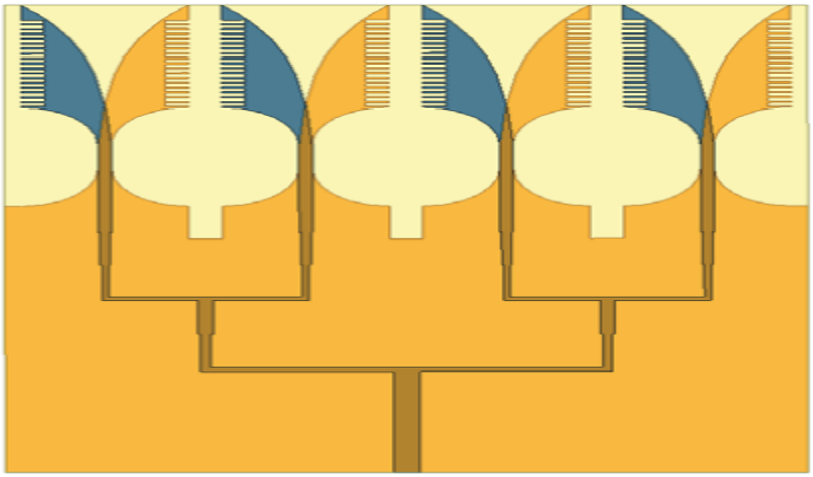

(b) Design of AVA array with corrugations (AVA-AC)

Fig. 1: Design of proposed AVA-AC (a & b)

$$C2 = e^{ax2}y21 - e^{ax1}/y1e^{ax2} - 1e^{ax1} \quad (3)$$

Here, $C1$ and $C2$ are constants, 'a' is a rate of increase of exponential curve. $x1$, $y1$, $x2$, and $y2$ are start and end points of exponential curve. The rate of increase of exponential curve for outer exponential curve is 0.7 and for inner curve is 1.5. Further, the start and end points of outer curve are $x1$ = 0, $y1$ = 3.2, $x2$ = 8.6, and $y2$ = 0.5. Also, the start and end points of inner curve are $x1$ = 0, $y1$ = 2.8, $x2$ = 2.35, and $y2$ = 0.5.

The corrugation introduces inductance and capacitance in an

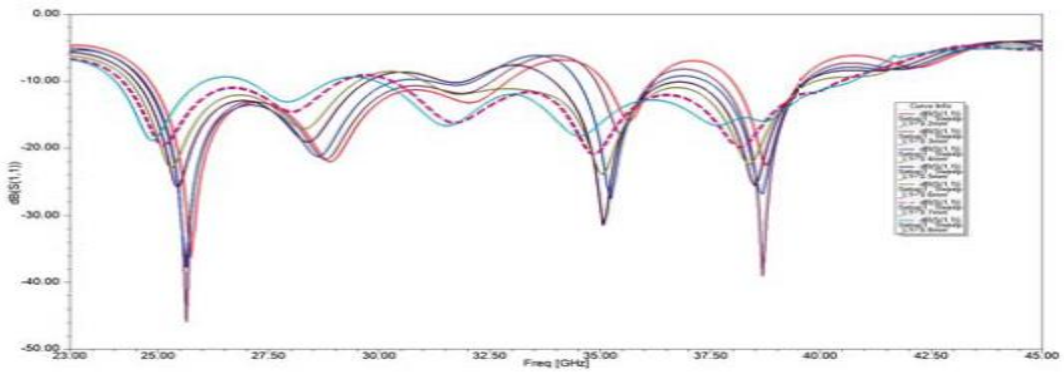

(a) Return loss for various lengths of corrugations

ISSN PRINT 2319 1775 Online 2320 7876
 Journal Volume 12, Iss 07, 2023

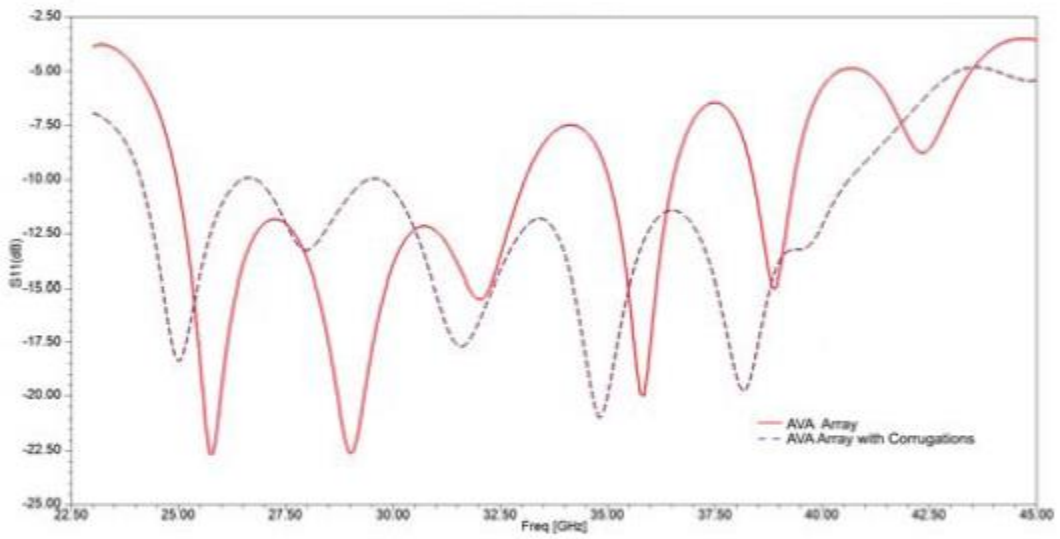

(b) Return loss of AVA-A and AVA-AC

Fig. 2: Return loss

antenna which in turn results in the change in its frequency repose. The return loss (S11) in dB for various dimensions of corrugations is shown in figure 2(a). This plots depicts that the best response is given for corrugation length 0.7 mm and width 0.2 mm as it provides wider bandwidth of 24.04 GHz to 40.85 GHz. Also, the S11 of initial AVA array and AVA array with corrugation (AVA-AC) is shown in figure 2(b). From this figure, it is proved that the operating frequency range of AVAAC is from 24.91 GHz to 33.18 GHz, 34.95 GHz to 36.58 GHz, and 38.34 GHz to 39.38 GHz which includes most of the frequency spectrum of 24.25 GHz to 27.5 GHz and 31.8 GHz to 33.4 GHz frequency bands of 5G communications. But, the second frequency band (34.95 GHz to 36.58 GHz) of AVA-A is not useful for 5G applications. This drawback of operating frequency range is overcome by incorporating corrugation in AVA array. The plot shown in figure 2(b) explains the importance of corrugation in the improvement of return loss. It shows that AVA-AC operates over 24.04 GHz to 40.85 GHz frequency range which includes three important bands of 5G communication spectrum which are 24.25 GHz

to 27.5 GHz, 31.8 GHz to 33.4 GHz, and 37 GHz to 40.5 GHz.

The feeding network is designed precisely to match 50Ω input impedance of SMA connector. Figure 3 shows the real and imaginary part of input impedance. This figure shows

ISSN PRINT 2319 1775 Online 2320 7876
 Journal Volume 12, Iss 07, 2023

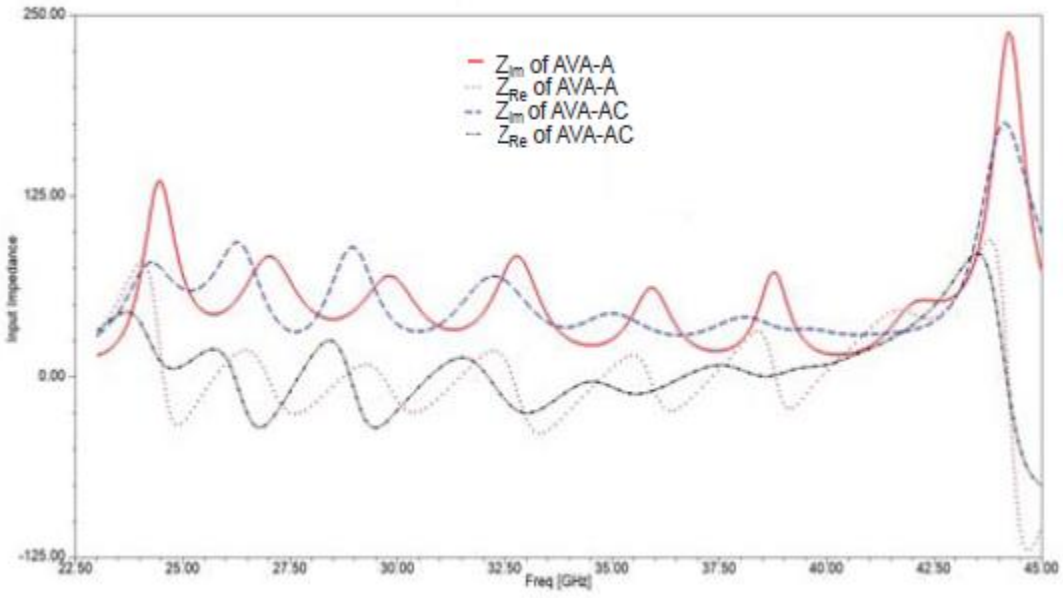

Fig. 3: Input impedance of AVA-A and AVA-AC

that AVA array feeding network provides nearly constant 50Ω input impedance in the frequency range of 24.04 GHz to 40.85 GHz. The dimensions of AVA array, corrugations, and antenna feeding network are optimized and then finalized. The various dimensions of AVA-AC are listed in table 1.

Parameters	Dimensions (mm)	Parameters	Dimensions (mm)
L1	24	W1	28
L2	6.3	W2	5
L3	5.4	W3	0.4
L4	2	W4	1
L5	2	W5	0.3
L6	2	W6	0.5
L7	2.04	W7	0.2
L8	6	W8	0.8

ISSN PRINT 2319 1775 Online 2320 7876
 Journal Volume 12, Iss 07, 2023

III. AVA-AC RESULTS

The designed AVA-AC is simulated by using HFSS version 19, simulation software. The E and H plane radiation patterns of AVA array and AVA-AC at 25 GHz, 31.6 GHz, and 38 GHz are shown in figure 4. This figure 4 proves that the design AVA-AC is the frequency independent as it provides stable radiation pattern. Also, it shows the reduction of back lobes after incorporating corrugations in AVA which in turn increases front to back ratio. Figure 5 is the plot of current distribution of AVA array and AVA-AC at 34 GHz. From figure, it can be seen that the current density of AVA array is weak at the flat edges which is boosted by corrugations.

Also, Corrugation increases electrical length and hence it is possible to reduce the antenna size. Further, the gain verses frequency is plotted in figure 6 which depicts that the gain of AVA array is in the range from 8.47 dB to 12.63 dB and the gain range of AVA-AC is from 8.2 dB to 13.2 dB. This proves that the corrugation enhances gain of an antenna form 12.63 dB to 13.2 dB and it helps to maintain the gain constant. To prove the importance of the proposed AVA-AC, its comparison with the existing AVA array is given in table 2. The table 2 proves that the proposed AVAAC is compact and it provides enhanced gain as compared

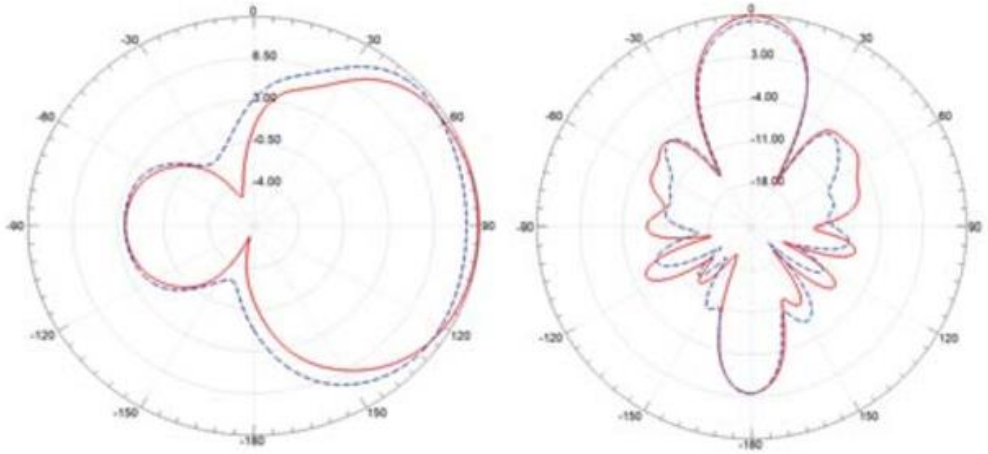

(a) (b)

ISSN PRINT 2319 1775 Online 2320 7876
 Journal Volume 12, Iss 07, 2023

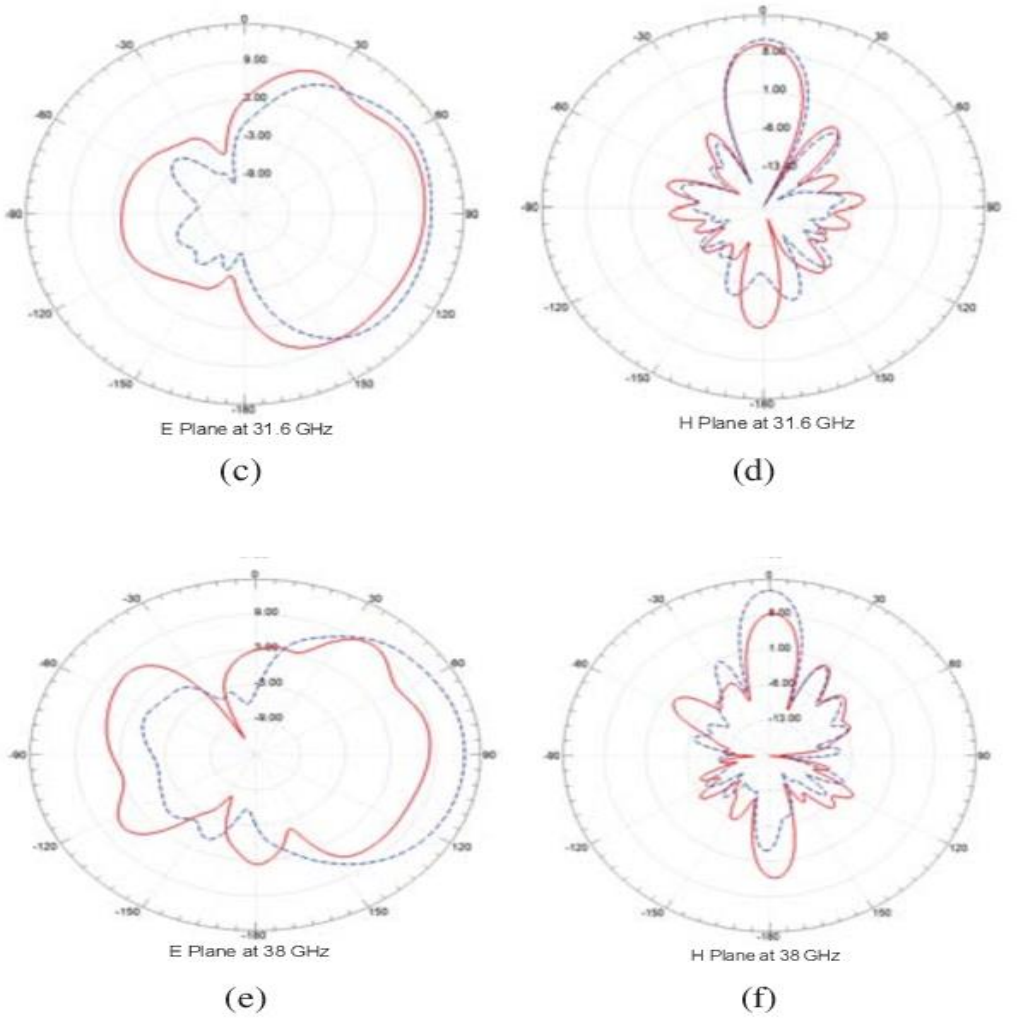

Fig. 4: E and H plane radiation patterns of AVA-A and AVAAC to other AVA array.

Further, operating frequency band of the proposed antenna is wider than the other AVA array. Hence the proposed antenna is suitable for 5G communication devices.

ISSN PRINT 2319 1775 Online 2320 7876
 Journal Volume 12, Iss 07, 2023

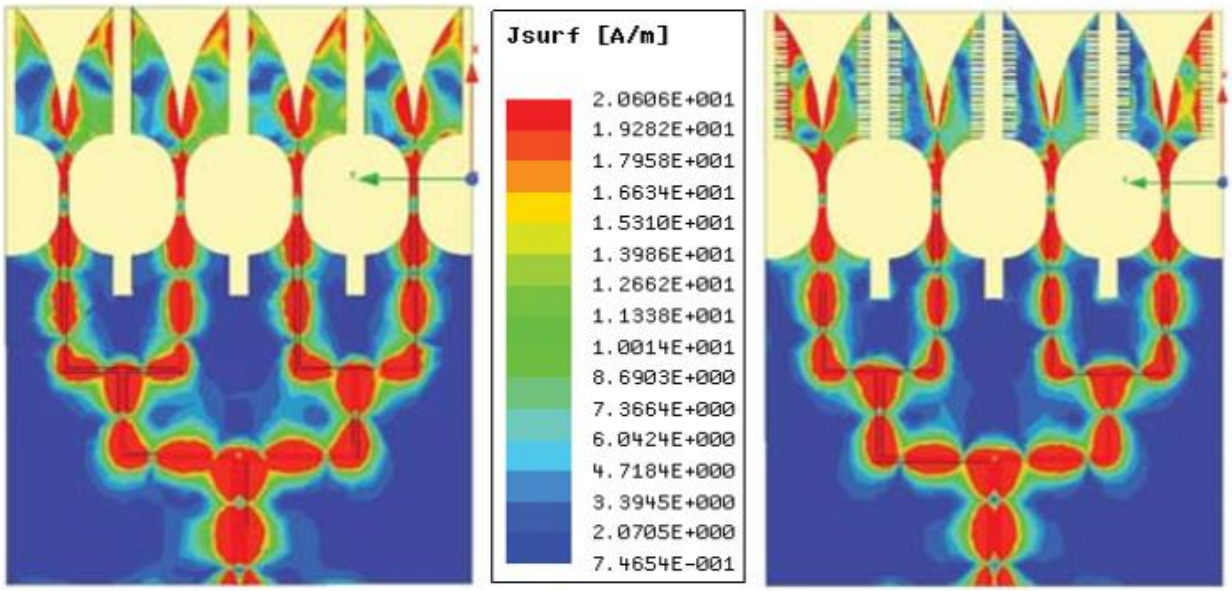

Fig. 5: Current distribution of AVA-A and AVA-AC

IV. CONCLUSION

The presented results of AVA-AC proves the importance of corrugations in AVA array for 5G communication applications. The design is finalized after optimizing the dimensions with help of HFSS software. The proposed AVA-AC enhances gain of AVA-A from 12.63 dB to 13.2 dB and increases the operating range to accommodate three frequency bands of 5G communication. Its operating frequency range is 24.04 GHz to 40.85 GHz frequency range which includes 24.25 GHz to 27.5 GHz, 31.8 GHz to 33.4 GHz, and 37 GHz to 40.5 GHz bands of 5G communication spectrum. Also, after incorporating corrugations in AVA array, back lobe level is reduced to a great extent which results in higher front to back ratio. As per the comprehensive review on AVA for 5G communication, the presented AVA-AC is the first antenna which is compact with enhanced gain and covers the first three bands of 5G communication. Hence, the proposed AVA-AC is the best antenna for upcoming 5G communication devices.

REFERENCES

[1] P. Gibson, “The Vivaldi Aerial,” *9th European Microwave Conference*, no. 1, pp. 101–105, 1979.

ISSN PRINT 2319 1775 Online 2320 7876
 Journal Volume 12, Iss 07, 2023

[2] E. Gazit, "Improved design of the Vivaldi antenna," *IEE Proceedings H Microwaves, Ant and Propag*, vol. 135, no. 2, p. 89, 1988.

[3] R. C. Deng, X. ming Yang, B. Ma, T. qian Li, H. yuan Chen, Y. Yang, H. He, Y. wen Chen, and Z. Tang, "Performance enhancement of novel antipodal Vivaldi antenna with irregular spacing distance slots and modified-w-shaped metamaterial loading," *Appl Phys A-Mater*, vol. 125, no. 5, pp. 1–11, 2019. [Online]. Available: http://dx.doi.org/10.1007/s00339-018-2298-6

[4] M. A. Boujemaa, R. Herzi, F. Choubani, and A. Gharsallah, "UWB Antipodal Vivaldi antenna with higher radiation performances using metamaterials," *Appl Phys A-Mater*, vol. 714, pp. 1–7, 2018. [Online]. Available: http://dx.doi.org/10.1007/s00339-018-2132-1

[5] P. J. Eichenberger, E. Yetisir, and N. Ghalichechian, "High-Gain Antipodal Vivaldi Antenna with Pseudoelement and Notched Tapered Slot Operating at 2.5-57 GHz," *IEEE Trans. Antennas Propag*, pp. 1–11, 2019.

[6] M. Moosazadeh, S. Kharkovsky, J. T. Case, and B. Samali, "Antipodal Vivaldi antenna with improved radiation characteristics for civil engineering applications," *IET Microw Antenna P*, vol. 11, no. 6, pp. 796– 803, 2017.

[7] A. Muniyasamy and K. Rajakani, "UWB radar cross section reduction in a compact antipodal Vivaldi antenna," *AEU – Int J Electron C*, vol. 99, pp. 369–375, 2019. [Online]. Available: https://doi.org/10.1016/j.aeue.2018.12.020

[8] P. Wang, H. Zhang, G. Wen, and Y. Sun, "Design of Modified 618 GHz Balanced Antipo- Dal Vivaldi Antenna," *Prog Electromagn Res C*, vol. 25, pp. 271–285, 2012.

[9] C. Sarkar, C. Saha, L. A. Shaik, J. Y. Siddiqui, and Y. M. M. Antar, "Frequency notched balanced antipodal tapered slot antenna with very low cross- polarised radiation," *IET Microw Antenna P Res*, vol. 12, no. 11, pp. 1859–1863, 2018.

[10] N. N. Wang, M. Fang, H. T. Chou, J. R. Qi, and L. Y. Xiao, "Balanced Antipodal Vivaldi Antenna with Asymmetric Substrate Cutout and Dual- Scale Slotted Edges for Ultrawideband Operation at Millimeter-Wave Frequencies," *IEEE Trans. Antennas Propag*, vol. 66, no. 7, pp. 3724– 3729, 2018.

[11] I. T. Nassar and T. M. Weller, "A Novel Method for Improving Antipodal Vivaldi Antenna Performance," *IEEE Trans. Antennas Propag*, vol. 63, no. 7, pp. 3321–3324, 2015.

ISSN PRINT 2319 1775 Online 2320 7876
 Journal Volume 12, Iss 07, 2023

[12] J. Bang, J. Lee, and J. Choi, "Design of a Wideband Antipodal Vivaldi Antenna with an Asymmetric Parasitic Patch," *Journal of Electromagnetic Engineering and Science*, vol. 18, no. 1, pp. 29–34, 2018.

[13] Y. Yao, X. Cheng, C. Wang, J. Yu, and X. Chen, "Wideband Circularly Polarized Antipodal Curvedly Tapered Slot Antenna Array for 5G Applications," *IEEE Journal on Selected Areas in Commun*, vol. 35, no. 7, pp. 1539–1549, 2017.

[14] B. Bhadoria and S. Kumar, "A Novel Omnidirectional Triangular Patch Antenna Array Using Dolph Chebyshev Current Distribution for C-Band Applications," *Progress In Electromagnetics Research M*, vol. 71, no. August, pp. 75–84, 2018.